Inter-diffusion across a direct p-n heterojunction of Li-doped NiO and Al-doped ZnO

Temesgen D. Desissa[§], Reidar Haugsrud[§], Kjell Wiik[‡], Truls Norby[§,*]

[§] *Department of Chemistry, Centre for Materials Science and Nanotechnology, University of Oslo, FERMiO, Gaustadalléen 21, NO-0349 Oslo, Norway*

[‡] *Department of Materials Science and Engineering, Norwegian University of Science and Technology (NTNU), NO-7491 Trondheim, Norway*

Abstract

We herein report inter-diffusion across the interface between p-type $Ni_{0.98}Li_{0.02}O$ and n-type $Zn_{0.98}Al_{0.02}O$ for various applications including p-n-heterojunction diodes and oxide thermoelectrics. Diffusion couples were made of polished surfaces of ceramic samples pre-sintered at 1250 and 1350 °C for $Ni_{0.98}Li_{0.02}O$ and $Zn_{0.98}Al_{0.02}O$, respectively. The inter-diffusion couples were annealed at 900 – 1200 °C for 160 h in ambient air. Electron Probe Micro Analysis (EPMA) was used to acquire diffusion profiles, followed by fitting to Fick's second law and Whipple-Le Claire's models for bulk and grain-boundary diffusion calculation, respectively. Zn^{2+} diffused into $Ni_{0.98}Li_{0.02}O$ mainly by bulk diffusion with an activation energy of 250±10 kJ/mol, whereas Ni^{2+} diffused into $Zn_{0.98}Al_{0.02}O$ by both bulk and enhanced grain boundary diffusion with activation energies of 320±120 kJ/mol and 245±50 kJ/mol, respectively. The amount of Al^{3+} diffused from the Al-doped ZnO into the NiO phase was too small for a corresponding diffusion coefficient to be calculated. Li-ion distribution and diffusivity were not determined due to lack of analyzer sensitivity for Li. The bulk and effective diffusivities of Zn^{2+} and Ni^{2+} into NiO and ZnO enable prediction of inter-diffusion lengths as a function of time and temperature, allowing estimates of device performance, stability, and lifetimes at different operation temperatures.

Keywords: NiO; ZnO; cation diffusion; grain-boundary diffusion; p-n junction

[*] *corresponding author, e-mail: truls.norby@kjemi.uio.no*

1. Introduction

Inter-diffusion plays a pivotal role in the stability and performance of high temperature p-n-junctions of semiconductor devices such as power electronics and thermoelectric generators where certain novel designs allow direct non-ohmic contacts between the p- and n-type materials[1-3]. NiO and ZnO are inherently p- and n-type semiconductors, respectively, with different crystal structures, having limited solid solubility, and forming no stoichiometric compounds. For the higher range of operating temperatures of these oxides, the solubility of NiO in ZnO is reported in the 1-5% range, while the solubility of ZnO in NiO is around 30%[3-5]. A p-n couple of materials with these two compositions across the miscibility gap will be in equilibrium with each other, which means that no inter-diffusion will take place if they are put in contact. However, if the two pure oxides are put in direct contact, there will be inter-diffusion until the formation of the equilibrium solid solutions. Moreover, if the equilibrated couple is exposed to a new temperature or a temperature gradient, equilibrium will be re-established by inter-diffusion.

The p- and n-type characters of NiO and ZnO are enhanced by doping with Li and Al, respectively, typically at levels of 1-2%, acting as acceptors and donors in the host oxides[6, 7]. The complete phase relationship comprising all four cation components has not been established to our knowledge. We assume, however, that Al and Li have some cross-solubility in NiO and ZnO, respectively, so that there will be inter-diffusion also of the dopants at the junction unless these are equilibrated or compositions adjusted from the beginning. Despite the range of applications of NiO-ZnO p-n junctions[8-10], there is little literature on cation inter-diffusion rates and mechanisms. Therefore, in the present work, these aspects have been investigated on diffusion couples made from $Ni_{0.98}Li_{0.02}O$ and $Zn_{0.98}Al_{0.02}O$ at 900 – 1200 °C.

2. Experimental procedures

Polycrystalline samples of $Ni_{0.98}Li_{0.02}O$ and $Zn_{0.98}Al_{0.02}O$ were synthesized by a standard solid-state chemical reaction route, using ≥ 99% purity chemicals of Li_2CO_3 (Sigma-Aldrich), NiO (Fuel Cell Materials, FCM), Al_2O_3 (Sigma-Aldrich), and ZnO (Sigma-Aldrich). Each pair of host and dopant precursors was weighed in their appropriate amounts and mixed in isopropanol, followed by ball milling for several hours. The mixture of Li_2CO_3 and NiO was calcined at 900 °C for 6 h and re-ground manually. The mixed powders were uniaxially pressed into pellets in a 20 mm diameter steel die. The Li-doped NiO and Al-doped ZnO were sintered at 1250 and 1350 °C, respectively, to reach relative densities estimated by weight and volume as well as by SEM images to be above 96%.

Powder X-ray diffraction (XRD) (Siemens Bruker D8 Discover) was used to verify phase purity of the samples.

The sintered samples were mounted in acetone dissolvable epoxy resin (Demotec 33, Germany) and the faces ground flat and polished down to 0.25 μm surface finish using diamond abrasive (DP-spray P, Struers, Denmark). Couples of the two materials were mounted with the polished surfaces facing each other in a ProboStat sample holder cell (NorECs, Norway) utilizing its spring-loaded alumina assembly system for fixing the samples and providing a dynamic mechanical load. The couples were annealed for inter-diffusion in ambient air at temperatures in the range of 900 – 1200 °C for a constant time of 160 h. The heating and cooling rate in all diffusion annealing experiments was set to 3 °C/min.

Current-voltage measurements were performed during annealing on one of the diffusion couples equipped with Pt paste electrodes using Agilent E3642A and 34970A instruments to supply a constant DC voltage and to measure the resulting current, respectively. Based on separate measurements, the electrical resistances and hence voltage losses of the bulk of the materials as well as the Pt contacts are negligible compared with that of the p-n-junction.

After annealing, each couple was held together by using a spring-load sample holder, cut perpendicular to the original interface using a diamond micro saw and mounted in an epoxy resin followed by grinding and polishing to a surface finish of 0.25 μm with the diamond abrasive. The samples were carbon coated (Emitech K950X) and subjected to diffusion profile analysis using Electron Probe Micro Analysis (EPMA, Cameca SX100) by applying 15 kV of acceleration voltage with a focused electron beam current of 20 nA. On each sample, diffusion profiles of 4 - 8 probing lines were acquired perpendicular to the initial interface. The individual profiles from the probing lines were combined to form one diffusion profile from which diffusion coefficients were calculated for Ni^{2+} and Zn^{2+} cations. X-ray elemental mappings were performed by EPMA to complement the diffusion profiles.

3. Results and discussion

3.1. Phase stability and diffusion mapping overview

XRD patterns confirmed that the end members remain single phase with no formation of any secondary phase due to doping or inter-diffusion. *Figure 1*(a) shows a backscattered electron (BSE) image of the junction with the corresponding elemental mapping of Ni^{2+} (b), Zn^{2+} (c) and Al^{3+} (d).

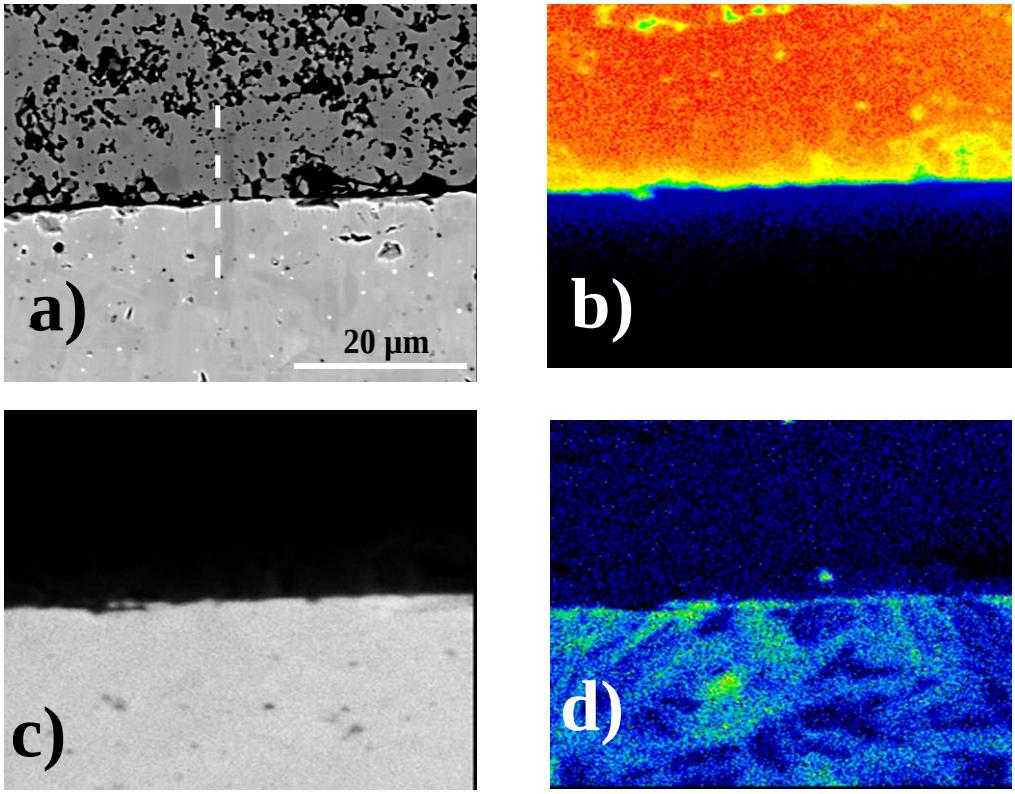

Figure 1. EPMA images of $Ni_{0.98}Li_{0.02}O$ (top) $Zn_{0.98}Al_{0.02}O$ (bottom) interface, showing the backscattered electron (BSE) microstructure (a) and EDS mappings of Ni (b), Zn (c), and Al (d) after the diffusion couple annealing at 1100 °C for 160 h. The dashed line in the BSE image indicates a typical probing line used to acquire a cation diffusion profiles.

As expected, the original phase boundary (interface) remained intact during the diffusion annealing, as seen in the BSE image. While the Al-doped ZnO (lower part) has remained dense, the p-type Li-doped NiO (upper part) appears more porous than it was as-sintered. We find no obvious reason for this based on the diffusion towards equilibrium solid solubilities, and do not elaborate on the matter in this contribution.

Close inspection of the lower part of *Figure 1* (b) reveals how Ni^{2+} diffused into the Al-doped ZnO via bulk but also enhanced in the grain boundaries, showing an essentially uniform inter-diffusion zone close to the initial interface and patterns of Ni^{2+} corresponding to the grain boundaries at a distance of approximately 10 µm away from the original interface into the Al-doped ZnO. In comparison, the penetration of Zn^{2+} into Li-doped NiO (*Figure 1* (c)) was shorter, with no sign of enhanced grain boundary diffusion.

In addition to Ni^{2+} and Zn^{2+} inter-diffusion, Al^{3+} exhibited diffusion into the Li-doped NiO phase (*Figure 1 (d)*), but the amount of Al^{3+} as analyzed by energy dispersive spectroscopy (EDS) of EPMA remained less than about 0.3 mole% in the NiO phase in the whole temperature range. The

Li-ion concentration was not mapped or analyzed due to the insufficient detection limit of the instrument for this element.

3.2. Grain (bulk) diffusion

The concentrations of diffusing species were measured using EPMA along lines of 40 to 100 μm length crossing the interface as exemplified in *Figure 1*(a). A representative inter-diffusion profile for the diffusion couple annealed at 1100 °C for 160 h built up of points from and representing an average of a number of individual probing lines is shown in *Figure 2*. It can be seen that the quantity of Ni^{2+} in ZnO starts below approximately 5 at. % whereas the quantity of Zn^{2+} in NiO starts below approximately 25 at. %, in qualitative agreement with the limited solid solubilities of the phases according to the phase diagram of the NiO-ZnO system [5].

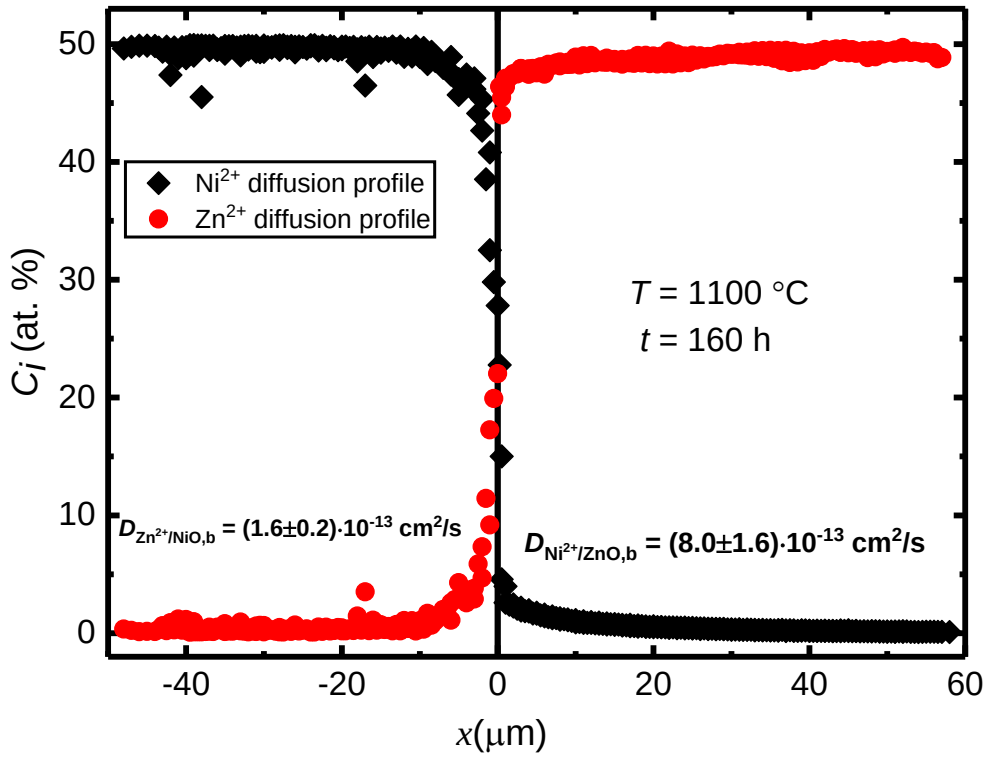

Figure 2. Diffusion profile of cations in the diffusion couple of $Ni_{0.98}Li_{0.02}O/Zn_{0.98}Al_{0.02}O$ annealed at 1100 °C for 160 h.

Bulk (lattice) inter-diffusion coefficients for each diffusing species, D_b, were determined from the solution of the Fick's second law of diffusion with boundary conditions of constant source, which reads [11-14]

$$C_i(x,t) = \frac{C_s - C_o}{2} erfc\left(\frac{x}{2\sqrt{D_b t}}\right) + C_o \qquad (1)$$

where $C_i\ (x,\ t)$ is the bulk concentration of diffusing species at distance x and annealing time t. C_s is the starting concentration at the source side, and C_o is the background concentration of the diffusing species at the sink side. Partial fitting was used for each cation on each side: The C_s was set to the maximum concentration of each cation at a distance, $x = 0$ towards their respective sink side. For example, the C_s was set to 5 at. % for bulk diffusion calculation of Ni^{2+} into ZnO and to 25 at. % for Zn^{2+} bulk diffusion into NiO. The calculated diffusivities are not very sensitive to the choice of the concentration of cations at $x = 0$. The calculated bulk inter-diffusivities at 1100 °C of Ni^{2+} and Zn^{2+} into ZnO and NiO, respectively, are $(8.0\pm1.6)\times10^{-13}$ cm^2/s and $(1.6\pm0.2)\times10^{-13}$ cm^2/s. An overview of results at other temperatures will be presented below.

3.3. Grain boundary diffusion

The grain boundary diffusion coefficient, $D_{gb,}$ can be expressed in terms of the grain boundary segregation factor (s), and grain boundary thickness (w) as given by the Whipple–Le Claire solution equation for a constant source [15, 16], which reads:

$$swD_{gb} = 0.3292\left(\frac{D_b}{t}\right)^{1/2}\left(-\frac{\delta\, log\, C}{\delta x^{6/5}}\right)^{-5/3} \quad (2)$$

D_b is the bulk or lattice diffusion coefficient as explained in equation (1), and the other parameters have their usual meanings. The grain boundary and bulk diffusion coefficients are related to the effective diffusion coefficient, D_{eff} through the Hart equation[17]:

$$D_{eff} = gD_{gb} + (1 - g)D_b \quad (3)$$

Here, g is volume fraction of the atomic site in the grain boundary given by $g \approx 3(w/d)$, where d is average grain size (≈ 10 μm) assuming the shape of the grain is cubic[18].

The contribution of the grain boundary concentration to the bulk can be written as[19]:

$$log\left(C_{x,gb}\right) = a + bx^{6/5} \quad (4)$$

Here, b is equivalent to the term $(-(\delta log(C)/\delta x^{6/5}))$ in Eq. (2). It is evident from *Figure 3* that $\log(C_i)$ against penetration depth $x^{6/5}$ exhibited a good linearity in the deepest region, referred to as the *grain boundary tail*, for Ni^{2+} diffusion into ZnO. Linear regression of the *grain boundary tail* according to Eq. (4) gives a slope from which b can be calculated. Using the obtained value of b back into Eq. (2), one can deduce the triple product, swD_{gb} from equation (2). Assuming 1 nm grain boundary thickness for Al-doped ZnO [20] and a segregation factor of unity, the grain boundary diffusion

coefficient can be calculated. On this basis, the calculated grain-boundary diffusion coefficient at 1100 °C was (1.3±0.1) ×10^{-7} cm^2/s.

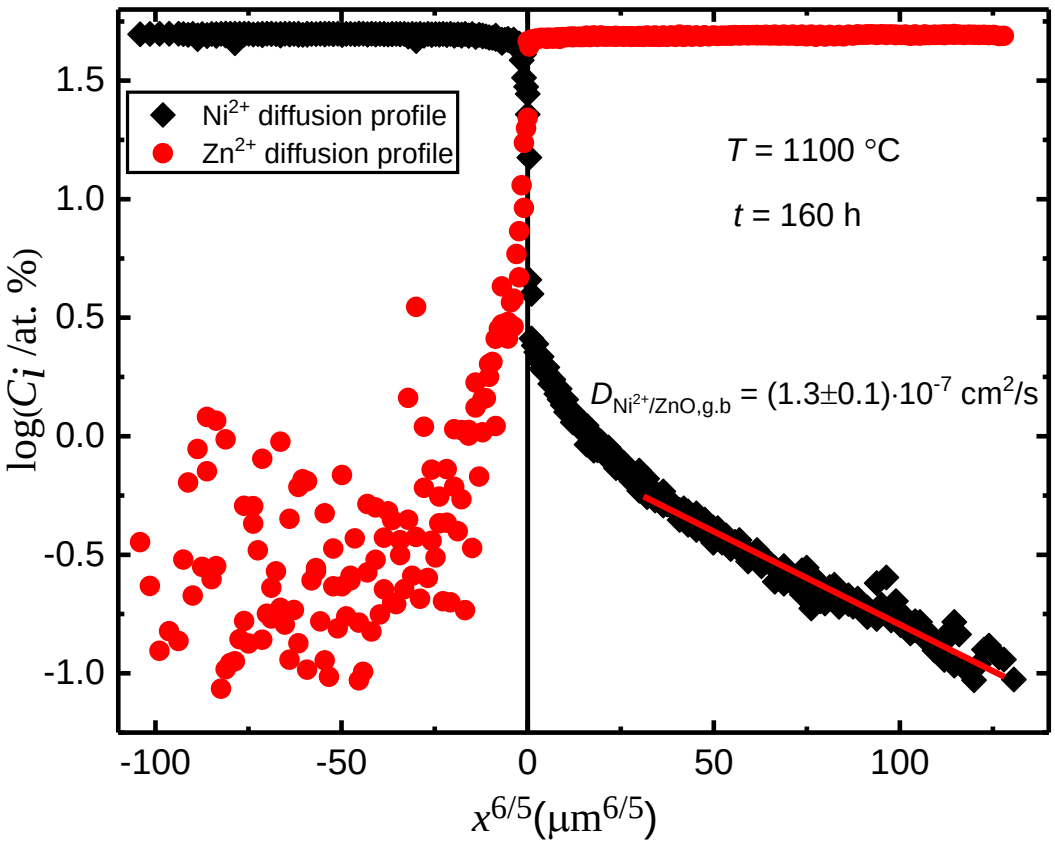

Figure 3. Plot showing a grain-boundary diffusion profile for the diffusion couple of $Ni_{0.98}Li_{0.02}O/Zn_{0.98}Al_{0.02}O$ annealed at 1100 °C for 160 h.

The deep region for Zn^{2+} remains scattered and shows no indication of enhanced grain boundary diffusion; Zn^{2+} transport in NiO is mainly governed by bulk diffusion, in accordance with the EDS mappings (cf. *Figure 1*).

Analysis of the Le Claire's critical parameters, β and α [18, 21] was used to categorize the diffusion kinetics of Ni^{2+} into ZnO as type B based on the criteria of $sw << (D_b t)^{1/2} << d$, with d of about 15 μm. In type B diffusion kinetics, the diffusion length is much smaller than the average grain size of the polycrystalline materials in addition to the ratio of the grain-boundary to bulk diffusion coefficient being much greater than unity [22]. The value of β, which is equivalent to $wD_{g.b}/(2D_b\sqrt{D_b t})$, varied from 550 at the lowest temperature to less than 10 at the highest temperature. On the other hand, α, which is equivalent to $sw/(2\sqrt{D_b t})$, changed from about 8×10^{-4} at the lowest temperature to about 4×10^{-5} at the highest temperature, indicating type B diffusion kinetics with enhanced grain-boundary diffusion of Ni^{2+} in Al-doped ZnO.

Figure 4 presents the diffusion profile of Al^{3+} after annealing at 1100 °C for 160 h. The concentration of Al^{3+} obtained was below the nominal initial dopant concentration in the Al-doped ZnO, assigned to the detection limit of the instrument. The quantity of Al^{3+} in Li-doped NiO was largely undetectable, and well below the Al solubility limit in NiO, according to the NiO-Al_2O_3 phase diagram [23]. On this basis, the profile for Al^{3+} was not significant enough to be fitted to a model, and hence the diffusion coefficient for Al^{3+} in NiO could not be calculated. However, the apparent absence of significant diffusion of Al^{3+} into NiO suggests that Al^{3+} diffuses slower than Zn^{2+} in NiO, which is reasonable based on the larger charge of Al^{3+}.

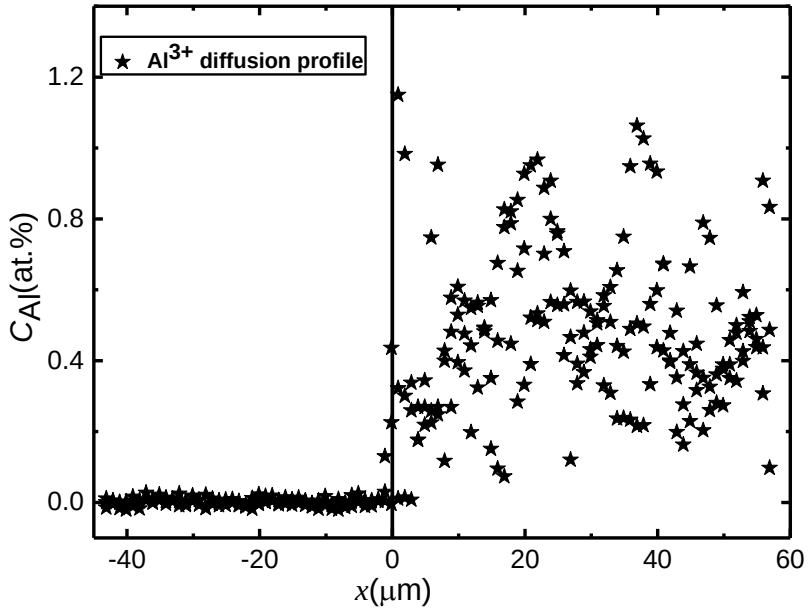

Figure 4. Diffusion profile of Al^{3+} obtained in the diffusion couple of $Ni_{0.98}Li_{0.02}O/Zn_{0.98}Al_{0.02}O$ annealed at 1100 °C for 160 h.

Figure 5 shows an Arrhenius plot of the calculated diffusion coefficients from the experiments in a temperature range of 900-1200 °C, along with linear fits to the equation.

$$D_i = D_o exp\left(\frac{-E_a}{RT}\right) \quad (5)$$

where, D_o is the pre-exponential factor, E_a is the activation energy, R is the gas constant, and T is the absolute temperature. The activation energy may consists of a defect formation enthalpy (ΔH_d°) and a defect migration enthalpy (ΔH_m)[24].

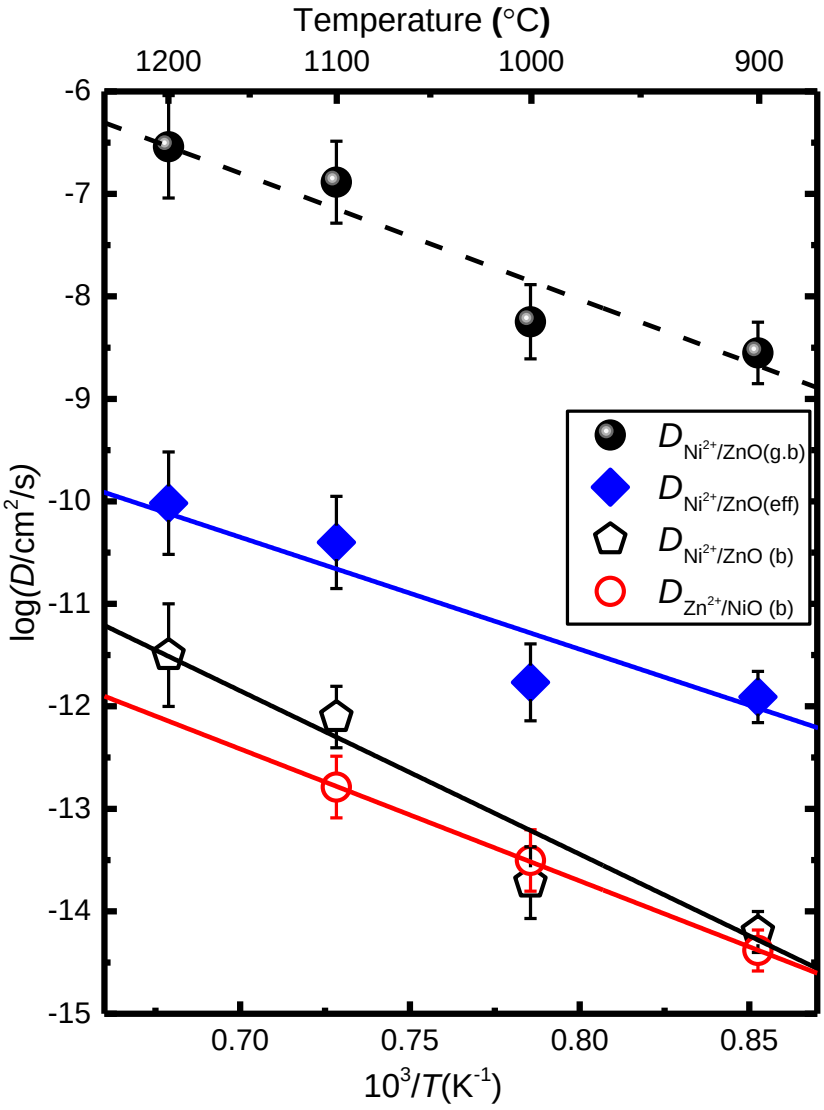

Figure 5. Arrhenius plot of diffusion coefficients for diffusion couples of $Ni_{0.98}Li_{0.02}O/Zn_{0.98}Al_{0.02}O$ with the solid lines representing linear fits and the bars indicating associated standard deviations.

The calculated pre-exponentials and activation energies including their statistical standard deviation confidence intervals from the regression are summarized in Equations (6-9):

$$D_{Zn^{2+}/NiO(b)} = 10^{-4.0\pm0.2}\exp\left(\frac{-250\pm10\ (\mathrm{kJ/mol})}{RT}\right)(\mathrm{cm}^2/\mathrm{s}) \quad (6)$$

$$D_{Ni^{2+}/ZnO(g.b)} = 10^{2\pm2}\exp\left(\frac{-250\pm50\ (\mathrm{kJ/mol})}{RT}\right)(cm^2/s) \quad (7)$$

$$D_{Ni^{2+}/ZnO(b)} = 10^{-1\pm2}\exp\left(\frac{-320\pm120\ (\mathrm{kJ/mol})}{RT}\right)(cm^2/s) \quad (8)$$

$$D_{Ni^{2+}/ZnO(eff)} = 10^{-3\pm2}\exp\left(\frac{-230\pm60\ (\mathrm{kJ/mol})}{RT}\right)(cm^2/s) \quad (9)$$

3.4. Comparison with data from literature

Despite the range of applications of the NiO-ZnO heterojunction such as in photo-electrochemistry [25, 26] and oxide based diodes[27], there is little literature on its interdiffusion. Nakagawa *et al.*[28] investigated the diffusion of Ni in ZnO using secondary ion mass spectrometry (SIMS) where the samples were prepared by thin film deposition of NiO on ZnO. The reported diffusion of Ni in ZnO was through both bulk and grain-boundaries, with activation energies of 306 and 292 kJ/mol, respectively, which largely agree with the present work. Additionally, Zn grain boundary diffusion in polycrystalline ZnO was investigated by Nogueira *et al.*[20] who reported an activation energy of 235 kJ/mol, again in agreement with the present work. Moore *et al.*[29] investigated Zn self-diffusion in polycrystalline ZnO in the early 1960s using ^{65}Zn radiotracer, obtaining a much smaller activation energy of 182 kJ/mol. Atkinson *et al.*[30] reported Ni bulk diffusion in NiO with activation energy of 243 kJ/mol corresponding well with our value for Zn diffusion in NiO. In another work [31] they reported 172 kJ/mol for grain-boundary diffusion of Ni in NiO, while we did not observe enhanced grain boundary diffusion of Zn in our NiO. The obtained diffusivities of the present work are shown in comparison to available literature data on similar materials in *Figure 6*.

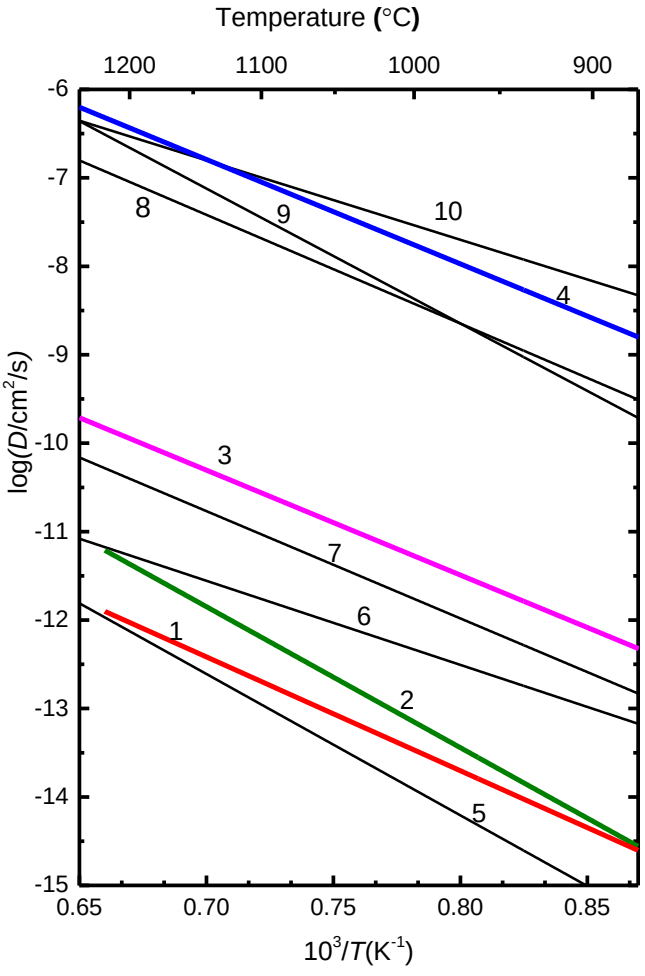

Figure 6. Comparison of bulk and grain-boundary diffusion coefficients: 1) Zn^{2+} bulk in Li-doped NiO (this work), 2) Ni^{2+} bulk in Al-doped ZnO(this work), 3) effective diffusion of Ni^{2+} in Al-doped ZnO (this work), 4) Ni^{2+} grain boundary in Al-doped ZnO(this work), 5) Ni^{2+} bulk in Al-doped ZnO[28], 6) Zn^{2+} bulk in ZnO[29], 7) Ni^{2+} bulk in NiO[30, 31], 8) Zn^{2+} grain boundary in ZnO[20], 9) Ni^{2+} grain boundary in ZnO [28], 10) Ni^{2+} grain boundary in NiO [31].

3.5. Effect of interdiffusion on junction electrical resistance

The rectifying function of a p-n junction at significant bias overpotentials is of interest for diode applications [27] while the resistance at open circuit and low overpotentials is of interest for use in thermoelectrics. These properties depend on several factors including band levels, charge carrier depletion, recombination, and thermal excitation of charge carriers. The resistance expectedly decreases with increasing temperature. One might expect that it also decreases as the junction during interdiffusion goes from the initial unmixed p-type Li-doped NiO and n-type Al-doped ZnO to the equilibrated compositions across the miscibility gap, where all cations are mixed. This probably reduces the differences and sharpness between band structures as well as the effective doping on both sides, and hence the purity of the p- and n-type character of the two materials across the junction, giving less charge carrier depletion and smaller resistance. While the matter deserves and is under continued investigation, we show in *Figure 7* that the resistance of the p-n junction as expected decreases during annealing at 1100 °C. This was obtained by taking isothermal voltage-current curves at different times and extracting the resistance as the derivative at zero current. A contribution from increasing contact area between the two oxides during annealing can not be excluded.

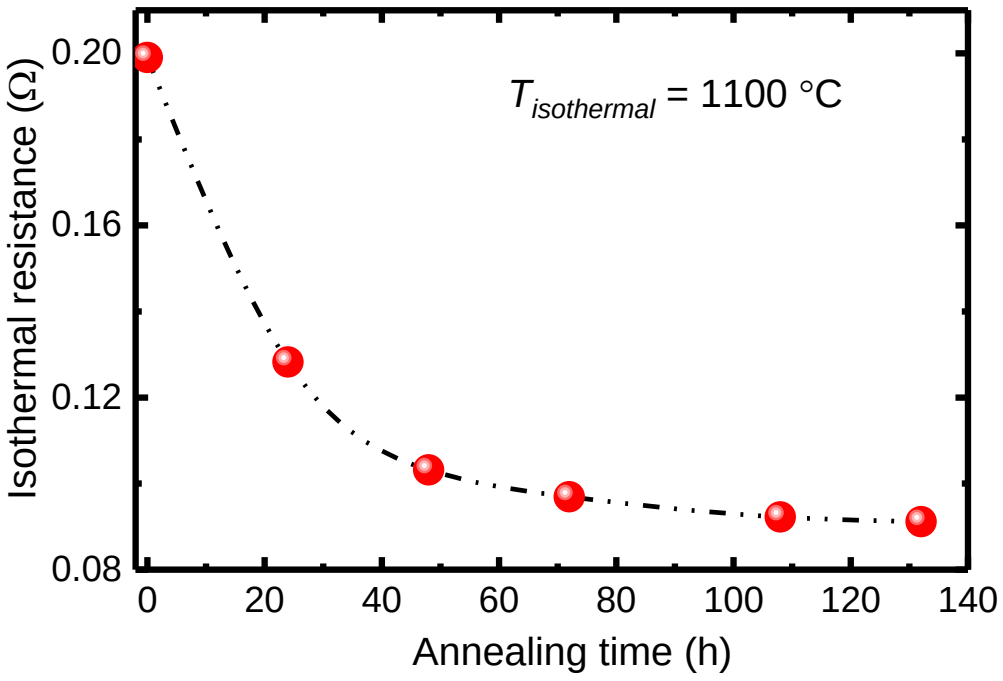

Figure 7. Isothermal resistance against annealing time of a $Ni_{0.98}Li_{0.02}O/Zn_{0.98}Al_{0.02}O$ diffusion couple at 1100 °C.

4. Summarizing conclusions

In summary, inter-diffusion has been investigated across a polycrystalline $Ni_{0.98}Li_{0.02}O/Zn_{0.98}Al_{0.02}O$ hetero-junction in the temperature range 900–1200 °C for 160 h in ambient air. As expected from the phase diagram, the junction remains stable, according to XRD, EDS, and EPMA. Bulk diffusion coefficients were calculated from the partial fitting of the inter-diffusion profiles to the appropriate solution to Fick's second law. Zn^{2+} bulk diffusion in Li-doped NiO had an activation energy of 250±10 kJ/mol whereas that of Ni^{2+} in Al-doped ZnO was 320±120 kJ/mol. Ni^{2+} transport into Al-doped ZnO exhibited enhanced grain boundary diffusion with an activation energy of 250±50 kJ/mol according to the Whipple–Le Claire model. Thus, grain boundary enhanced diffusion dominates the effective diffusivity of Ni^{2+} in polycrystalline ZnO.

Annealing at 1100 °C decreases the electrical resistance of the junction, tentatively assigned to the levelling out of cation contents and band structure resulting from the interdiffusion.

The obtained diffusivities allow prediction of the depth and effects of inter-diffusion as a function of time and temperature during fabrication and operation processes. Ni^{2+} diffusion into ZnO would be about 200 µm at 900 °C over a period of five years, while Zn^{2+} under the same conditions would diffuse about 20 µm into NiO. One may on this basis suggest that practical higher temperature operation of direct NiO-ZnO junctions must be held well below 900 °C, unless a total equilibration of the two stable compositions is desired. Our study showed on the other hand that inter-diffusion for a few hours even at 1100 °C (for processing and fabrication) may be tolerable, and for some applications like direct p-n-junctions in thermoelectrics be beneficial.

Acknowledgements

The authors acknowledge the Research Council of Norway (RCN) for financial support under the "THELMA" project (228854) of the Nano2021 program and Dr. M. Erambert at the Department of Geoscience, the University of Oslo, for EPMA analysis.

References

[1] G. Span, M. Wagner, T. Grasser, L. Holmgren, *phy. stat. sol. (RRL)* **1** (2007) (6) 241-243.

[2] R. Chavez, A. Becker, V. Kessler, M. Engenhorst, N. Petermann, H. Wiggers, G. Schierning, R. Schmechel, *MRS Proc. Libr.* **1543** (2013) 3-8.

[3] H. Kurokawa, M. Nanko, K. Kawamura, T. Maruyama, *Stability and Electrical Properties of High Temperature p-n Junction of NiO-ZnO System*, J. Electrochem. Soc., Pennington, N.J. (2001).

[4] D.-S. Sinn, *Solid State Ionics* **83** (1996) (3–4) 333-348.

[5] C.H. Bates, W.B. White, R. Roy, *J. Inorg. Nucl. Chem.* **28** (1966) (2) 397-405.

[6] F.J. Morin, *Phys. Rev.* **93** (1954) (6) 1199-1204.

[7] P.H. Miller, *Phys. Rev.* **60** (1941) (12) 890-895.

[8] B. Yin, Y. Qiu, H. Zhang, Y. Chang, D. Yang, L. Hu, *RSC Advances* **6** (2016) (54) 48319-48323.

[9] J.-J. Liang, M.-G. Zhao, L.-J. Ding, S.-S. Fan, S.-G. Chen, *Chin. Chem. Lett.* **28** (2017) (3) 670-674.

[10] Z.-F. Shi, T.-T. Xu, D. Wu, Y.-T. Zhang, B.-L. Zhang, Y.-T. Tian, X.-J. Li, G.-T. Du, *Nanoscale* **8** (2016) (19) 9997-10003.

[11] J. Crank, *The mathematics of diffusion*, Oxford university press (1979).

[12] J.B. Smith, T. Norby, A. Fossdal, *J. Am. Ceram. Soc.* **89** (2006) (2) 582-586.

[13] N. Čebašek, R. Haugsrud, T. Norby, *Solid State Ionics* **231** (2013) 74-80.

[14] P.G. Shewmon, *Diffusion in solids*, McGraw-Hill (1963).

[15] R.T.P. Whipple, *The London, Edinburgh, and Dublin Philosophical Magazine and Journal of Science* **45** (1954) (371) 1225-1236.

[16] A.D.L. Claire, *Br. J. Appl. Phys.* **14** (1963) (6) 351.

[17] E.W. Hart, *Acta Metall.* **5** (1957) (10) 597.

[18] H. Mehrer, *Diffusion in Solids: Fundamentals, Methods, Materials, Diffusion-Controlled Processes*, Springer Berlin Heidelberg, Berlin, Heidelberg (2007), p.209-236.

[19] E. Vøllestad, T. Norby, R. Haugsrud, *Solid State Ionics* **244** (2013) 57-62.

[20] M.A.d.N. Nogueira, W.B. Ferraz, A.C.S. Sabioni, *Materials Research* **6** (2003) 167-171.

[21] D. Gaertner, G. Wilde, S.V. Divinski, *Acta Mater.* **127** (2017) 407-415.

[22] H. Mehrer, *Diffusion in Solids: Fundamentals, Methods, Materials, Diffusion-Controlled Processes*, Springer Berlin Heidelberg, Berlin, Heidelberg (2007), p.553-582.

[23] B. Phillips, J.J. Hutta, I. Warshaw, *J. Am. Ceram. Soc.* **46** (1963) (12) 579-583.

[24] N. Čebašek, R. Haugsrud, T. Norby, *Solid State Ionics* **254** (2014) 32-39.

[25] C. Zhang, W. Fan, H. Bai, X. Yu, C. Chen, R. Zhang, W. Shi, *ChemElectroChem* **1** (2014) (12) 2089-2097.

[26] Z. Zhang, C. Shao, X. Li, C. Wang, M. Zhang, Y. Liu, *ACS Appl. Mater. Interfaces* **2** (2010) (10) 2915-2923.

[27] M. Grundmann, R. Karsthof, H. von Wenckstern, *ACS Appl. Mater. Interfaces* **6** (2014) (17) 14785-14789.

[28] T. Nakagawa, I. Sakaguchi, K. Matsunaga, T. Yamamoto, H. Haneda, Y. Ikuhara, *Nucl. Instrum. Methods Phys. Res.* **232** (2005) (1–4) 343-347.

[29] W.J. Moore, E.L. Williams, *Discuss. Faraday Soc.* **28** (1959) (0) 86-93.

[30] A. Atkinson, R.I. Taylor, *J. Mater. Sci.* **13** (1978) (2) 427-432.

[31] A. Atkinson, R.I. Taylor, *Philos. Mag. A* **43** (1981) (4) 979-998.